IChemE
0957–5820

Trans IChemE, Vol 76, Part B, May 1998

PROPAGATION OF LAMINAR FLAMES IN WET PREMIXED NATURAL GAS-AIR MIXTURES

B. Z. DLUGOGORSKI, R. K. HICHENS, E. M. KENNEDY and J. W. BOZZELLI*

Department of Chemical Engineering, The University of Newcastle, New South Wales, Australia
**Department of Chemical Engineering, Chemistry and Environmental Sciences, New Jersey Institute of Technology, New Jersey, USA*

The present work investigates the effect of adding small amounts of humidity on the inhibition of natural gas-air flames. The inhibition is quantified by measuring and calculating the laminar burning velocities (S_u) of premixed flames from a C_1-C_2 mechanism. The experimental apparatus consists of a Mache-Hebra burner, equipped with flow controllers and air purification system. Steam is generated by injecting water into a preheated natural gas-air stream, by means of a syringe pump. The burning velocities are determined experimentally from the schlieren photography using the total flame area.

The results indicate decreasing burning velocities with increasing steam concentration, demonstrating the importance of thermal capacity of water vapour on slowing down the flame propagation. There is no indication of flame acceleration due to kinetic considerations, even when the flames are doped with minute moisture loadings. It is shown in the calculations that the laminar burning velocity depends strongly on the number of grid points, and so a scaling relationship is developed for adjusting the computed values of S_u. The kinetic model predicts closely the experimental results, but the agreement between the experimental and numerical data is better at lower temperatures. The relationship between S_u and the concentration of the added water vapour, as calculated from the model, is linear. For the natural gas considered in this work, the laminar burning velocity at the atmospheric pressure decreases by 1.81 cm s^{-1} at 150°C for each percentage point of humidity present in the gas mixture, and by 1.18 cm s^{-1} at 20°C.

Keywords: laminar burning velocities; mitigation of fires and explosions; inerting of flammable mixtures with water vapour.

INTRODUCTION

With the compulsory phase-out of halons, and the ongoing replacement of some of the existing halon-based fire-suppression systems with water-mist systems, it is often assumed that water mist can be safely used in industrial installations which are exposed to explosion hazards because of the existence of a flammable-gas mixture. This situation may occur, for example, on offshore platforms when a water-mist system is activated immediately prior to an explosion. Unfortunately, recent experimental results indicate that water mist, while being very effective on fires, has an undesirable property of accelerating explosion waves, under certain conditions[1]. From this perspective, questions have been raised whether the acceleration is physical in nature—that is, due to the turbulence induced by the injected water mist—or whether it results from a chemical process such as variations in radical concentrations because of the added humidity[2]. The objective of the present work is to measure and calculate the laminar burning velocities to determine which effect predominates. Natural gas, commonly encountered in petroleum and chemical industries, is chosen for this investigation, rather than methane.

The literature related to the acceleration of the propagating explosion waves by water mist is at best confusing. The work of Thomas and Brenton[3], which follows earlier studies of Carlson *et al.*[4], indicates an acceleration of methane deflagration, induced by the application of water mist. These deflagration results are corroborated in the detonation regime by Tsarichenko *et al.*[5] who observe that the presence of a film of water on the walls of the explosion tube intensifies the combustion process leading to the faster rise in the detonation overpressure. On the other hand, several publications, for example that of Acton *et al.*[6], report results of water sprays restricting flame speeds, and reducing the magnitude of overpressures. Other workers, such as Catlin *et al.*[7], note the ambivalent effect of water sprays on explosions; under one set of experimental conditions, the sprays mitigate the explosions whereas the altered conditions lead to more violent explosions with higher overpressures. The present investigation will show that the wet-flame chemistry of natural gas-air combustion cannot account for the observed acceleration in the propagation of the explosion waves.

The next two sections introduce the experimental and computational methodologies, including the chemical kinetic model used in the computation. This is followed

by the description and discussion of the measured and predicted values of the laminar burning velocities in wet premixed natural gas-air flames.

EXPERIMENTAL SET-UP

In the present work, we employ a conical Mache-Hebra type nozzle burner[8] in conjunction with the total surface area measurement using the schlieren photography technique, to establish the laminar burning velocity at atmospheric pressure. The area of the cold gas-cone surface immediately before the flame, as needed for the calculations, is obtained by dividing the schlieren area (a_s) by a correction factor of 1.11, which is recommended by Andrews and Bradley[9]. The mixture of flammable gases is preheated in the furnace before the burner and in the burner itself to collect the experimental data at elevated temperatures of up to 150°C, as shown in Figure 1. The velocity of the gases flowing through the Mache-Hebra nozzle (v) is adjusted for this heating using the ideal gas law. The laminar burning velocity (S_u) is obtained from the following expression:

$$S_u = 1.11\frac{va}{a_s} \quad (1)$$

where a stands for the cross-sectional area of the torch nozzle.

The Mache-Hebra burner allows for the existence of a straight-sided stabilized-flame cone by generating a uniform velocity profile across the nozzle[9]. In the Mache-Hebra burner, strain rate and flame curvature are minimized by maintaining the ratio of the visible flame height to nozzle diameter to below three[10]. This is because the heating of the flammable gases before combustion (due to the interaction of the jet with the surrounding gas) engenders a buoyancy force which modifies the uniform velocity profile. Note that, other workers recommend that the nozzle is operated at even shorter flame heights. For example, Linteris and Truett[11] keep the ratio at a constant value of 1.3 in their experiments.

Following Liu and MacFarlane[12], we use stainless steel for fabrication of the nozzle burner and note that flames show no apparent curvature because of this choice of torch material. Our burner is 200 mm in length and 44 mm in inside diameter at the base. The nozzle is 10 mm in diameter and the contraction occurs over a distance of 32 mm. The contraction surface is traced by the axisymmetric surfaces with radii of curvature of 22 and 20 mm, respectively. The torch has no nitrogen gas shroud shield, as the fuel equivalence ratios investigated in this study (up to 1.4) are well below that (1.7) for which the secondary heating, due to the formation of the diffusion cone, was found to influence the premixed burning[13]. Glass beads fill part of the torch to reduce fluctuations of the cone and the thermocouple is inserted for temperature control of the incoming gases. The furnace evaporates the water injected into the stream of a dried natural gas-air mixture and heats the gases to a pre-set temperature. A mass flow controller and a rotameter maintain the predetermined flow rates of natural gas and air, respectively. Finally, our schlieren set-up follows similar arrangements developed by Caldwell *et al.*[10] and van Wonterghem and van Tiggelen[14].

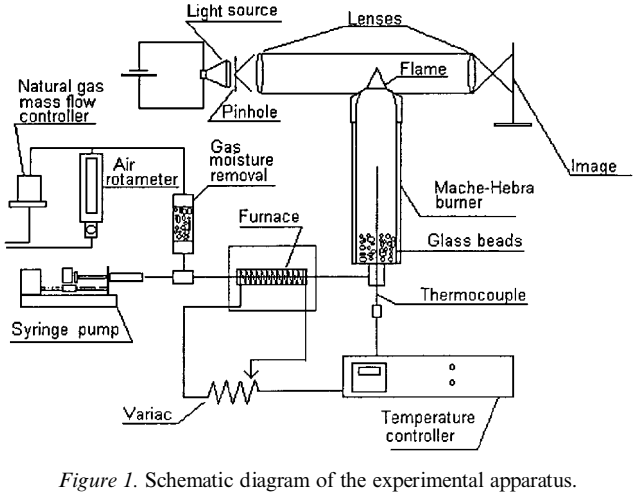

Figure 1. Schematic diagram of the experimental apparatus.

The composition of the natural gas is given in Table 1. The components whose concentrations fall below 0.001% are not included in the table. For the purpose of modelling, the residual oxygen and argon are added to nitrogen, and all hydrocarbons are distributed among methane and ethane in such a way as to maintain the same consumption of oxygen. Since various hydrocarbons release almost the same amount of heat with respect to the amount of the oxygen consumed in the combustion process[15], this redistribution of the hydrocarbons allows the application of the C_1-C_2 mechanism in the modelling, and preserves the heat that would have been produced from the oxidation of the original natural gas.

MODELLING AND KINETIC MECHANISM

The flame structure and the burning velocities are obtained from the Sandia steady one-dimensional Premix code[16] for modelling the planar propagation of the premixed laminar flames. The present paper contains only the data for the laminar burning velocities, although the code also calculates the variation in the species concentrations across the flame zone. The Premix code solves the conservation equations for mass, species and energy at constant pressure and assumes adiabatic flames. This means that the losses due to radiation from the flame and due to conduction between the flame and the torch, as occurring in the experimental apparatus, are neglected. The code relies on the gas phase libraries, provided with the Chemkin-II distribution[17], for the calculation of kinetic rates as well as thermodynamic and transport coefficients. We execute the Premix code using mixture-average transport coefficients in conjunction with the corrected diffusion velocity. The convection terms are handled with the windward

Table 1. Composition of the desiccated natural gas used in the present study.

Gas	Comp, %	Comp, % adjusted
O_2/Ar	0.06	–
N_2	1.23	1.29
CH_4	88.89	87.79
CO_2	1.88	1.88
C_2H_6	7.59	9.04
C_3H_8	0.14	–
C_4H_{10}	0.21	–

differencing scheme and the Soret (thermal) diffusion is switched off. The calculations yield accelerating flames and the laminar burning velocity, to be compared with the experimental measurement, is obtained at the inlet of the premixed gases.

The kinetic model used in the present work incorporates the C_2 mechanism to allow for the production of C_2 molecules from CH_3 radicals and to account for the relatively high ethane content of our natural gas. This is especially important in the case of fuel-rich flames, where half to two thirds of methane reactions proceed along the C_2 pathway[18]. The mechanism is illustrated in Table 2 and with the exception of reaction number 79, whose kinetic constants are taken from Baulch *et al.*[19], is based on the mechanism developed by Ho and Bozzelli[20], Ho *et al.*[21–23] and Booty *et al.*[24] for studying the combustion and pyrolysis of hydrochlorocarbon-doped systems. In particular, the papers by Ho *et al.*[21,22] and Ho and Bozzelli[20] contain tables and other references indicating how the mechanism was completed, validated and used, and how the rate constants were either calculated from QRRK theory or evaluated and obtained from other sources.

The calculations carried out by Premix, as part of the boundary conditions, use vanishing gradients at some distance away downstream from the combustion zone. The approach of the flame temperature, in this zone of vanishing gradients, to the adiabatic flame temperature, provides only an approximate indication of the convergence of the laminar burning velocity S_u to its ultimate value. This is because the magnitude of the laminar burning velocity is very sensitive to the number of grid points used in the calculations. This number is regulated by GRAD and CURV parameters within the Premix code. We decreased the value of these parameters down to 0.01, unless the number of grid points allowed (NMAX) exceeded 1250, in subsequent executions of the computer code. Figure 2 illustrates that S_u scales proportionally with the reciprocal number of grid points N, that is according to:

$$S_u = S_u(N) - \frac{\alpha(\phi)}{N} \tag{2}$$

where the proportionality constant α depends on the fuel equivalence ratio ϕ. For fuels considered in this article, this dependence can be cast into the following expression: $\alpha(\phi) = 100(-1.80 + 3.90\phi - 1.82\phi^2)$. Note that the relationship presented in equation (2) applies for $N > 50$.

The fact that the laminar burning velocity calculated by Premix tends to decrease with increasing grid density was also observed by others—for example, Linteris and Truett[11]. In the calculations carried out in the present paper, we populated the computational domain with more than 1000 nodes. From Figure 2 or equation (2), this means that the values of S_u reported in the next chapter are higher by no more than 0.7% than those in the limit of $1/N$ approaching zero.

RESULTS AND DISCUSSION

Figure 3 compares laminar burning velocities of methane-air mixtures as measured experimentally by Andrews and Bradley[26] and Liu and MacFarlane[12] with the prediction of the present kinetic model. These former experimental results are widely accepted and often used as benchmarks. For methane-air combustion, our model predicts the maximum burning velocity to be about 3% higher than that obtained by Linteris and Truett[11]. It is clear that the difference between the measured[12,26] and calculated (present work) values of the maximum burning velocity is of the order of 10%. Had we chosen other experimental data sets, such as that of Vagelopoulos *et al.*[27], we would have obtained perfect agreement. This observation stresses that the predictions from our model reproduce the laboratory data as closely as it is currently possible given the scatter among various experimental data sets.

Also observe that the model predicts higher laminar burning velocities for the natural gas containing a significant amount of ethane, than for methane alone. This observation follows one's intuition, since ethane is more reactive than methane due to methane's strong C-H bonds, engendering faster laminar burning velocities. Clearly at 20°C, the model reproduces the maximum S_u to within 1.5 cm s^{-1} and the agreement between the computed results and the experimental data is even better for both fuel-rich and lean flames.

In order to investigate the applicability of the model at the elevated temperatures of the premixed gases, we carried out experiments at 100, 150 and 200°C followed by detailed chemical-kinetic computations. The results, illustrated in Figures 4 and 5, are important from the practical perspective when mixtures of hydrocarbons are processed (or mixed by accident) together with air at higher temperatures. This creates additional hazards as the burning velocity increases significantly with the temperature[26]. The present model reproduces exactly the laminar burning velocities for natural gas-rich flames over the entire range of temperatures investigated in this work. However, the experiments show higher S_u at high temperatures and at stoichiometric and low fuel equivalence ratios, than determined from model calculations. Although this is satisfactory, the model needs further refinement.

The growing difference between the computational and experimental data, with increasing temperatures of the incoming gases, is further illustrated in Figure 5. In that figure, we replot S_u at the fuel equivalence ratio of 1.1 (as interpolated from Figure 4) and compare this with the model prediction and with the empirical equation of Andrews and Bradley[26]:

$$S_u = 10 + 0.000371T^2, \tag{3}$$

where S_u is in cm s^{-1} and T in K.

Strictly speaking, the correlation of Andrews and Bradley applies to methane at the fuel equivalence ratio of 1.0, and is included in the present figure for comparison. This correlation provides more accurate predictions than the model, but it is applicable only at the maximum laminar burning velocity of the dry natural gas, approximated as methane. The model underpredicts the experimental S_u by up to 10% at 200°C—that is, at the highest temperature investigated in this study. However, the model provides the versatility needed for calculating S_u of the mitigated flames, as illustrated in Figures 6 and 7.

The data presented here include experiments with the addition of a very small amount of humidity (0.15%), in Figure 6, followed by the calculation of the maximum burning velocity of mitigated flames at the fuel equivalence

Table 2. Detailed C_1-C_2 mechanism for combustion of natural gas-air reaction system as used in this work; $k = A\,T^b\,e^{-E/RT}$. Rota *et al.*[25] have recently compared the predictions from other commonly used C_1-C_2 kinetic mechanisms for modelling combustion of methane-ethane mixtures in perfectly stirred tank reactors. The activation energies originally expressed in cal mol^{-1} have been converted to SI units of J mol^{-1}, and we have kept all digits before the decimal point for consistency in the conversion.

No	Reaction	A, mol cm^{-1} s^{-1}K	b	E, J mol^{-1}
1	$C_2H_6 = C_2H_5 + H$	6.22E+47	−9.8	465,470.0
2	$C_2H_6 + CH_3 = C_2H_5 + CH_4$	2.70E−01	4.0	34,644.0
3	$C_2H_6 = CH_3 + CH_3$	5.34E+54	−11.1	469,487.0
4	$C_2H_6 + H = C_2H_5 + H_2$	6.61E+13	0.0	15,062.0
5	$C_2H_6 + O = C_2H_5 + OH$	2.51E+13	0.0	26,778.0
6	$C_2H_6 + OH = C_2H_5 + H_2O$	8.85E+19	1.0	7,573.0
7	$C_2H_5 = C_2H_4 + H$	1.83E+39	−7.8	220,999.0
8	$C_2H_5 + CH_3 = CH_4 + C_2H_4$	5.50E+11	0.0	0.0
9	$C_2H_5 + H = CH_3 + CH_3$	1.35E+22	−2.2	29,288.0
10	$C_2H_5 + O = CH_2O + CH_3$	1.00E+13	0.0	0.0
11	$C_2H_5 + O_2 = C_2H_4 + HO_2$	2.00E+12	0.0	20,887.0
12	$C_2H_5 + HO_2 = C_2H_4 + H_2O_2$	3.01E+11	0.0	0.0
13	$C_2H_5 + CH_3O = C_2H_6 + CH_2O$	2.41E+13	0.0	0.0
14	$C_2H_5 + CH_2O = CHO + C_2H_6$	5.50E+03	2.8	24,518.0
15	$C_2H_4 = C_2H_3 + H$	8.53E+30	−5.9	494,716.0
16	$C_2H_4 = C_2H_2 + H_2$	8.52E+43	−8.3	507,268.0
17	$C_2H_4 + OH = C_2H_3 + H_2O$	1.58E+04	2.8	17,460.0
18	$C_2H_4 + CH_3 = CH_4 + C_2H_3$	4.20E+11	0.0	46,497.0
19	$C_2H_4 + O_2 = C_2H_3 + HO_2$	4.22E+13	0.0	241,095.0
20	$C_2H_4 + H = C_2H_3 + H_2$	6.92E+14	0.0	60,668.0
21	$C_2H_3 = C_2H_2 + H$	6.24E+29	−5.3	194,556.0
22	$C_2H_3 + O_2 = C_2H_2 + HO_2$	1.21E+11	0.0	0.0
23	$C_2H_3 + O_2 = CHO + CH_2O$	3.97E+12	0.0	−1046.0
24	$C_2H_2 + O_2 = C_2H + HO_2$	1.21E+13	0.0	311,792.0
25	$C_2H_2 + O = CO + CH_2$	4.10E+08	1.5	7,113.0
26	$C_2H_2 + O = HCCO + H$	1.02E+07	2.0	7,950.0
27	$C_2H_2 + OH = C_2H + H_2O$	1.45E+04	2.7	50,375.0
28	$C_2H_2 + OH = CH_2CO + H$	3.20E+11	0.0	837.0
29	$C_2H + O_2 = CO + CHO$	2.41E+12	0.0	0.0
30	$C_2H + H_2 = C_2H_2 + H$	1.15E+13	0.0	12,050.0
31	$C_2HCH_4 = C_2H_2 + CH_3$	1.81E+12	0.0	2,092.0
32	$C_2H + OH = CH_2 + CO$	1.81E+13	0.0	0.0
33	$C_2H + OH = C_2H_2 + O$	1.81E+13	0.0	0.0
34	$HCCO + H = CH_2s + CO$	3.00E+13	0.0	0.0
35	$CH_2CO + O = CH_2 + CO_2$	1.74E+12	0.0	5648.0
36	$CH_2CO + H = HCCO + H_2$	5.00E+13	0.0	33,472.0
37	$CH_2CO + O = HCCO + OH$	1.00E+13	0.0	33,472.0
38	$CH_2CO + OH = HCCO + H_2O$	7.50E+12	0.0	8,368.0
39	$CH_2CO + M = CH_2 + CO + M$	3.00E+15	0.0	317,900.0
40	$CH_2CO + OH = CHO + CH_2O$	2.80E+13	0.0	0.0
41	$CH_2CO + H = CH_3CO$	1.50E+04	2.8	2815.0
42	$CH_2s + M = CH_2 + M$	1.00E+13	0.0	0.0
43	$CH_2s + O_2 = CO + H_2O$	2.41E+11	0.0	0.0
44	$CH_2s + CH_4 = C_2H_5 + H$	9.43E+12	−0.1	27,698.0
45	$CH_2s + CH_4 = CH_3 + CH_3$	3.45E+22	−2.5	31,213.0
46	$CH_2s + CH_4 = C_2H_6$	5.78E+46	−10.3	53,681.0
47	$CH_2s + H_2 = CH_4$	3.82E+25	−4.5	15,774.0
48	$CH_2s + H_2 = CH_3 + H$	1.27E+14	−0.1	544.0
49	$CH_4 = CH_3 + H$	1.03E+33	−5.6	467,813.0
50	$CH_4 + H = CH_3 + H_2$	1.55E+14	0.0	46,024.0
51	$CH_4 + O_2 = CH_3 + HO_2$	4.04E+13	0.0	238,111.0
52	$CH_4 + O = CH_3 + OH$	1.02E+09	1.5	35,982.0
53	$CH_4 + OH = CH_3 + H_2O$	1.93E+05	2.4	8,828.0
54	$CH_4 + HO_2 = CH_3 + H_2O_2$	2.00E+13	0.0	75,312.0
55	$CH_3 + O_2 = CH_2O + OH$	3.59E+09	−0.1	42,468.0
56	$CH_3 + O_2 = CH_3O + O$	2.88E+15	−1.1	129,076.0
57	$CH_3 + O = CH_2O + H$	7.00E+13	0.0	0.0
58	$CH_3 + OH = CH_3O + H$	3.87E+12	−0.2	57,492.0
59	$CH_3 + HO_2 = CH_3O + OH$	2.00E+13	0.0	0.0
60	$CH_3 + CH_2O = CH_4 + CHO$	1.00E+11	0.0	25,481.0
61	$CH_3O + O_2 = CH_2O + HO_2$	6.62E+10	0.0	10,878.0
62	$CH_3O + M = CH_2O + H + M$	1.00E+14	0.0	105,018.0
63	$CH_3O + CO = CO_2 + CH_3$	1.57E+13	0.0	49,371.0
64	$CH_3O + HO_2 = CH_2O + H_2O_2$	3.01E+11	0.0	0.0
65	$CH_3O + CH_3 = CH_4 + CH_2O$	2.41E+13	0.0	0.0
66	$CH_3O + O = OH + CH_2O$	6.03E+12	0.0	0.0
67	$CH_3O + OH = H_2O + CH_2O$	1.81E+13	0.0	0.0
68	$CH_3O + H = CH_2O + H_2$	1.99E+13	0.0	0.0
69	$CH_3O + CH_2 = CH_3 + CH_2O$	1.81E+13	0.0	0.0

Table 2. (Continued)

No	Reaction	A, mol cm^{-1} s^{-1}K	b	E, J mol^{-1}
70	$CH_2O + H = CHO + H_2$	2.50E+13	0.0	16,694.0
71	$CH_2O + O = CHO + OH$	3.50E+13	0.0	14,686.0
72	$CH_2O + OH = CHO + H_2O$	3.00E+13	0.0	4,979.0
73	$CH_2O + HO_2 = CHO + H_2O_2$	1.00E+12	0.0	33,472.0
74	$CH_2O + M = CHO + H + M$	5.00E+16	0.0	318,821.0
75	$CH_2O + O_2 = CHO + HO_2$	2.05E+13	0.0	162,946.0
76	$CH_2 + CH_4 = CH_3 + CH_3$	1.82E+05	0.0	0.0
77	$CH_2 + H_2 = CH_3 + H$	3.01E+09	0.0	0.0
78	$CH_2 + H_2O = CH_3 + OH$	9.64E+07	0.0	0.0
79	$CH_2 + O_2 = CH_2O + O$	1.00E+14	0.0	15,481.0
80	$CHO + M = H + CO + M$	2.50E+14	0.0	70,249.0
81	$CHO + = CO + H_2$	2.00E+14	0.0	0.0
82	$CHO + O_2 = CO + HO_2$	5.12E+13	0.0	7071.0
83	$CHO + O = CO + OH$	3.01E+13	0.0	0.0
84	$CHO + O = H + CO_2$	3.01E+13	0.0	0.0
85	$CHO + OH = CO + H_2O$	3.01E+13	0.0	0.0
86	$CO + OH = CO_2 + H$	4.40E+06	1.5	-3100.0
87	$CO + HO_2 = CO_2 + OH$	5.80E+13	0.0	95,956.0
88	$CO + O_2 = CO_2 + O$	2.50E+12	0.0	199,995.0
89	$CO + O + M = CO_2$	6.17E+14	0.0	12,552.0
90	$H + O_2 = O + OH$	1.69E+17	−0.9	72,760.0
91	$H + O_2 + M = HO_2 + M$	1.42E+18	−0.8	0.0
92	$H + H_2O = H_2 + H$	4.60E+08	1.6	77,655.0
93	$H + OH + M = H_2O + M$	7.50E+23	−2.6	0.0
94	$H + O + M = OH + M$	2.29E+14	0.0	16,318.0
95	$H + HO_2 = OH + OH$	1.69E+14	0.0	3,640.0
96	$H + HO_2 = H_2 + O_2$	6.62E+13	0.0	8,912.0
97	$H + H_2O_2 = H_2 + HO_2$	4.82E+13	0.0	33,263.0
98	$H + H_2O_2 = OH + H_2O$	2.41E+13	0.0	16,610.0
99	$H_2 + M = H + H + M$	4.57E+19	−1.4	436,768.0
100	$H_2 + O = H + OH$	1.08E+04	2.8	24,769.0
101	$O + H_2O = OH + OH$	1.50E+10	1.1	72,132.0
102	$O + H_2O_2 = HO_2 + OH$	9.63E+06	2.0	16,610.0
103	$O + HO_2 = OH + O_2$	2.00E+13	0.0	0.0
104	$OH + HO_2 = H_2O + O_2$	2.00E+13	0.0	0.0
105	$OH + H_2O_2 = HO_2 + H_2O$	1.75E+12	0.0	1339.0
106	$O_2 + M = O + O + M$	1.20E+14	0.0	449,998.0
107	$O_2 + H_2O_2 = HO_2 + HO_2$	5.42E+13	0.0	166,272.0
108	$H_2O_2 + M = OH + OH + M$	1.29E+33	−4.9	222,798.0

ratio of 1.1, in Figure 7. This small level of humidity was selected to provide a possible reservoir of H and OH radicals without affecting substantially the heat capacity of the incoming gas mixtures. Within the experimental uncertainty, we have observed no acceleration of the burning velocities, and the detailed chemical kinetics modelling has yielded S_u declining by less than 0.3 cm s^{-1} upon addition of 0.15% of water vapour. This reduction in S_u is well within the experimental uncertainty and cannot be detected with the present experimental equipment.

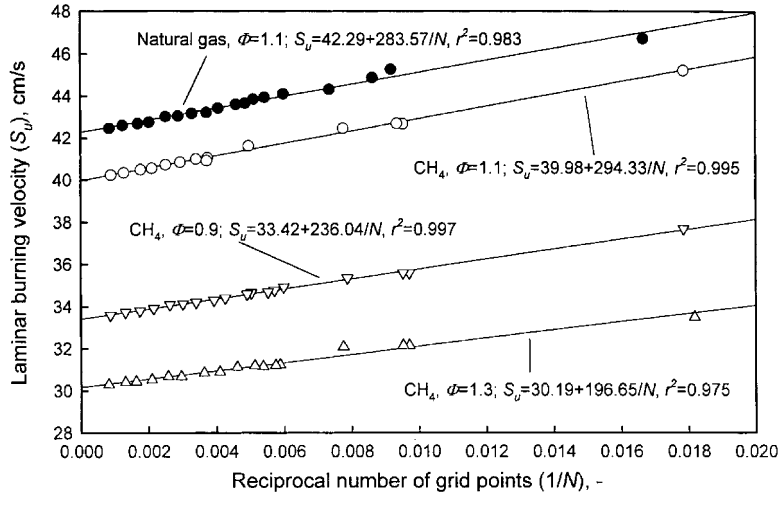

Figure 2. The effect of grid density on the computed values of the laminar burning velocity.

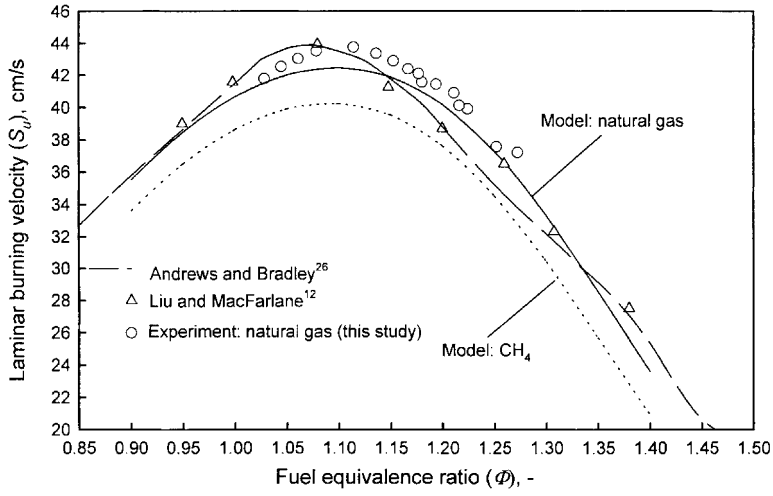

Figure 3. The comparison among various sets of experimental and computational results of methane and natural-gas laminar burning velocities, at 20°C and atmospheric pressure.

To quantify the efficiency of mitigation of the natural gas flames with the addition of humidity, we define the inerting coefficient c_i as:

$$c_i = -\frac{1}{S_u}\frac{\partial S_u}{\partial H_{H_2O}} \tag{4}$$

From Figure 7, it follows that the inerting coefficient declines from 0.0270 to 0.0244 $\%_{H_2O}^{-1}$ between 20 and 150°C, respectively. This means that the humidity inerts flammable mixtures more efficiently at lower temperatures of the incoming gases. Although a detailed analysis of the reaction paths including radical production and consumption rates is yet to be carried out, the present results suggest that the effect of water vapour on modifying the chemistry of natural gas-air flames, to lead to faster laminar burning velocities, is not significant. That is, the added water vapour acts as a heat sink, since its thermal capacity (on volume or molar basis) is higher than other gases entering the combustion zone.

For the fuel-lean flames this observation is not as surprising as for the fuel-rich flames. As the fuel equivalence ratio decreases below unity, the combustion process is essentially complete. In this regime, the burning velocity relates to the adiabatic flame temperature, which depends on the heat of reaction and the heat capacity of gases participating in the combustion[26,28,29]. On the other hand, in the fuel-rich regime, we initially surmised that the addition of humidity would enhance burning and accelerate the laminar burning velocities. This hypothesis came from the prior observations by Hives and Smith[30] that water mist injected into the combustion chamber of diesel engines improves combustion efficiency thus yielding higher power output, and from those of Atreya *et al.*[31] who have described small-scale combustion experiments, in which the combustion efficiency increased in the presence of water mist.

From the fundamental perspective, the slowing down of fuel-rich flames reflects the production of hydrocarbons due to the incomplete combustion. These hydrocarbons act as

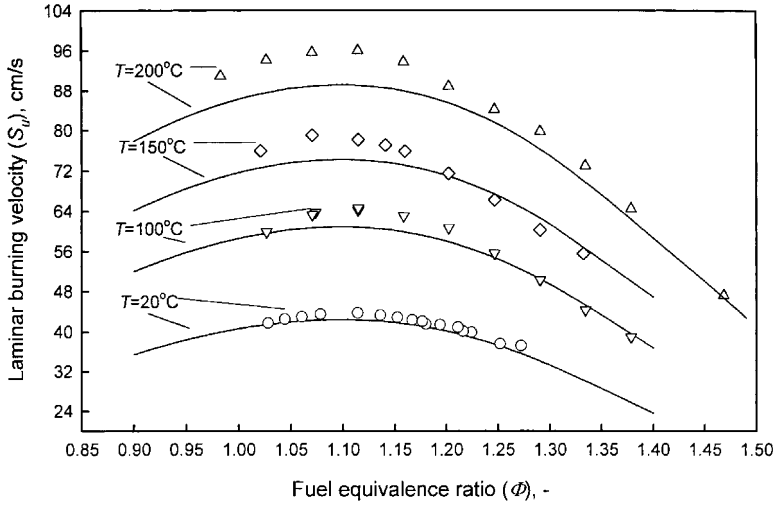

Figure 4. The effect of temperature and the fuel equivalence ratio on the laminar burning velocities of dry natural gas; the gas composition is listed in Table 1. Symbols correspond to the experimental results and solid lines denote predictions of the kinetic model.

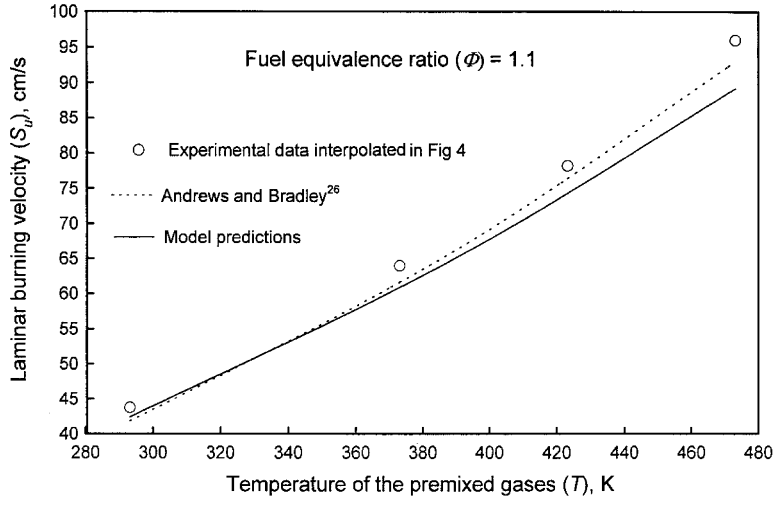

Figure 5. The variation of the laminar burning velocity with increasing temperature at atmospheric pressure. Symbols and solid lines relate to experimental and computational results for natural gas (Table 1) at the fuel equivalence ratio of 1.1.

scavengers of radicals, especially oxygen radicals, by the following routes[18]:

$$C_2H_2 + O \rightarrow CH_2 + CO \quad \text{and} \quad CH_3 + O \rightarrow CH_2O + H$$

The oxygen radical concentration is restored in two fast reactions at the cost of net radical consumption according to[18]:

$$H + OH \rightarrow H_2 + O \quad \text{and} \quad OH + OH \rightarrow H_2O + O$$

The addition of small quantities of water vapour does not seem to slow down significantly the second reaction $OH + OH \rightarrow H_2O + O$, which produces only one O radical for each two consumed radicals of OH. It is very implausible that the addition of more water vapour than investigated in this work, would lead to the acceleration of burning velocities. This is because at larger concentrations of water vapour, the physical effect of humidity as a heat sink will likely dominate any catalytic effect, producing a net decrease in the propagation of the laminar premixed flames.

Finally, we would like to make a comment about the relative importance of chemical and physical (thermodynamic) effects of adding water vapour on the laminar burning velocity, at higher concentrations of H_2O[32]. One can conveniently carry out an evaluation of these effects by performing calculations in which water vapour is not allowed to participate in chemical reactions. In addition, the physical effect itself contains contributions due to dilution of the reacting mixtures by water vapour and due to the role of water vapour as a sink for the heat generated in the combustion process. Magnitudes of these contributions can be further separated in the calculations by neglecting the thermal capacity of water vapour. Figure 8 illustrates the results from these computations. Note an insignificant chemical suppression and the variation of the dilution and thermal capacity effects with the addition of water vapour.

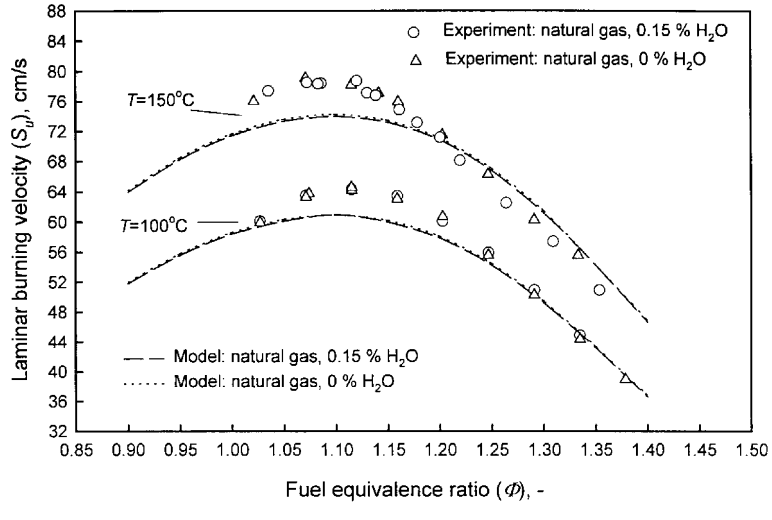

Figure 6. The comparison between experimental and calculated laminar burning velocities of natural gas (Table 1) with and without the addition of a small amount of water vapour.

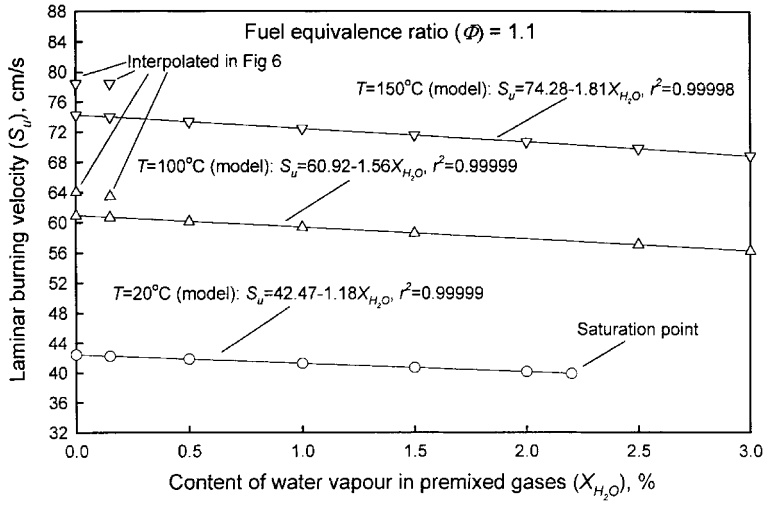

Figure 7. The effect of diluting the mixture of natural gas and air with water vapour on the laminar burning velocity, at the fuel equivalence ratio of 1.1 and at atmospheric pressure. This figure contains mainly numerical results. The four points interpolated from the experimental data (Figure 6) are included for comparison.

CONCLUSIONS

The reaction mechanism, listed in Table 2, has been applied to predict the laminar burning velocities of ethane-rich natural gas-air flames in the presence of humidity. Detailed chemical-kinetic modelling carried out in conjunction with experimental investigation demonstrates that the effect of humidity on S_u is mostly thermal even at very low concentrations of water vapour in the premixed gases. For example, the experimental data obtained at 100 and 200°C with (0.15% H_2O) and without water vapour indicate essentially the same values of the laminar burning velocities, within the experimental uncertainty. This means that the observed acceleration of explosion waves in the presence of activated water-mist fire-suppression systems cannot be explained by a chemical-kinetic argument and must therefore follow from physical considerations, such as water-mist induced turbulence.

The results of computations of S_u exhibit excellent agreement with the laboratory measurements, especially at the lower temperatures. On the other hand, at the elevated temperatures, and for stoichiometric and fuel-lean flames, the agreement lessens but remains within 10%. The laminar burning velocity displays a strong sensitivity to the number of grid points, decreasing on the insertion of additional nodes. The paper shows that a good estimate of the laminar burning velocity can be obtained by taking S_u to be inversely proportional to the number of grid points.

The addition of water vapour always tends to decrease the laminar burning velocities in mixtures of natural gas and air and the paper introduces the inerting coefficient to quantify this observation. The inerting coefficient compares the rate of change of S_u, with the addition of the inerting agent, with S_u itself. From the modelling study, for the addition of small amounts of water vapour at the fuel equivalence ratio of 1.1, this coefficient varies between 0.0270 to 0.0244, at 20 and 150°C respectively, indicating that the natural gas-air mixtures are inerted more efficiently at lower temperatures. This means that the laminar burning velocity decreases more significantly at the

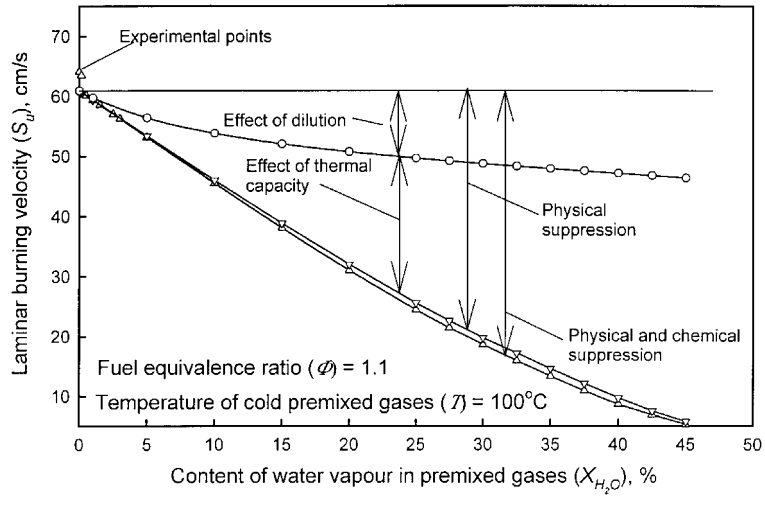

Figure 8. The influence of dilution, thermal capacity of water vapour and chemical kinetics on the laminar burning velocity[32].

higher temperatures. For example, at 150°C S_u decreases by 1.81 cm/(s $\%_{H_2O}$), whereas at 20°C S_u is reduced by 1.18 cm/(s $\%_{H_2O}$).

NOMENCLATURE

A	pre-exponential factor, mol cm^{-1} s^{-1} K^{-1}
a	cross-sectional area of the torch nozzle, cm^2
a_s	area of the schlieren cone, cm^2
b	temperature exponent in the rate constant
c_i	inerting coefficient in equation (4), $\%_{H_2O}^{-1}$
E	activation energy, J mol^{-1}
k	rate coefficient, mol cm^{-1} s^{-1}
N	number of grid points
R	universal gas constant, 8.314 J mol^{-1} K^{-1}
S_u	laminar burning velocity, cm s^{-1}
T	temperature, K or °C
v	velocity of gases flowing through the Mache-Hebra nozzle, cm s^{-1}
X	mole fraction (–) or volume percent (%)

Greek symbols

ϕ	fuel equivalence ratio, $(X_f/X_{O_2})/(X_f/X_{O_2})_{stoich}$
α	proportionality constant in equation (2)

Subscripts

f, H_2O, O_2	denotes fuel, water and oxygen, respectively

REFERENCES

1. Jones, A. and Thomas, G. O,, 1993, The action of water sprays on fires and explosions: A review of experimental work, *Trans IChemE,* 71 (B2): 41–9.
2. van Wingerden, K., Wilkins, B., Bakken, J. and Pedersen, G., 1995, The influence of water sprays on gas explosions: 2. Mitigation, *J Loss Prev Proc Ind,* 8 (2): 61–70.
3. Thomas, G. O. and Brenton, J. R., 1994, A study of turbulent flame acceleration in water sprays, *HSE OTH Report, OTH94 463* (ISBN 0 7176 1118 3).
4. Carlson, L. W., Knight, R. M. and Henrie, J. O., 1973, Report, Atomics International Division, Rockwell International, Canoga Park CA, USA.
5. Tsarichenko, S. G., Shebeko, Y. N., Trunev, A. V., Zaitsev, A. A. and Kaplin, A. Y., 1993, Flame propagation in hydrogen air mixtures in a tube, *Comb Explos & Shock Waves*, 29 (6): 674–8.
6. Acton, M. R., Sutton, P. and Wickens, M. J., 1990, An investigation of the mitigation of gas cloud explosions by water sprays, *IChemE Symp Ser, No 122*, 61-76.
7. Catlin, C. A., Gregory, C. A. J., Johnson, D. M. and Walker, D. G., 1993, Explosion mitigation in offshore modules by general area deluge *Trans IChemE*, 71 (B1): 101–11.
8. Mache, H. and Hebra, A., 1941, Zur Messung der Vebrennungsgeschwindigkeit explosiver Gasgemische, *Akademie der Wissenschaft (Wien) Sitzungsberichte IIa*, 150 (1-10): 157–74.
9. Andrews, G. E. and Bradley, D., 1972, Determination of burning velocities: A critical review, *Comb & Flame*, 18: 133–53.
10. Caldwell, F. R., Broida, H. P. and Dover, J. J., 1951, Combustion in Bunsen flames, *Ind Eng Chem*, 43 (12): 2731–9.
11. Linteris, G. T. and Truett, L., 1996, Inhibition of premixed methane-air flames by fluoromethanes, *Comb & Flame*, 105: 15–27.
12. Liu, D. D. S. and MacFarlane, R., 1983, Laminar burning velocities of hydrogen-air and hydrogen-air-steam flames, *Comb & Flame*, 49: 59–71.
13. Byrne, J. F., 1953, The influence of atmospheric oxygen on Bunsen flames, *Proc 4th Symp (Int) on Comb*, 345–8.
14. van Wonterghem, J. and van Tiggelen, A., 1951, L˝epaisseur et la vitesse de propagation du front de flamme, *Bull Soc Chim Belg*, 63: 235–60.
15. Thornton, W. M., 1917, The relation of oxygen to the heat of combustion of organic compounds, *Phil Mag*, 33: 196–203.
16. Kee, R. J., Grcar, J. F., Smooke, M. D. and Miller, J. A., 1985, *A Fortran Computer Program for Modeling Steady Laminar One-Dimensional Premix Flames, SAND85-8240* (Sandia National Laboratories Report).
17. Kee, R. J., Rupley, F. M. and Miller, J. A., 1989, *Chemkin-II: A Fortran Chemical Kinetics Package for the Analysis of Gas Phase Chemical Kinetics, SAND89-8009B* (Sandia National Laboratories Report).
18. Levy, J. M., Taylor, B. R., Longwell, J. P. and Sarofim, A. F., 1982, C_1 and C_2 chemistry in rich mixture, ethylene/air flames, *Proc 19th Symp (Int) on Comb,* 167-79.
19. Baulch, D. L., Cobos, C. J., Cox, R. A., Frank, P., Hayman, G., Just, Th., Kerr, J. A., Murrells, T., Pilling, M. J., Troe, J., Walker, R. W. and Warnatz, J., 1994, Evaluated kinetic data for combustion modelling: Supplement I, *J Phys Chem Ref Data*, 23 (6): 847–1033.
20. Ho, W. P. and Bozzelli, J. W., 1992, Validation of a mechanism for use in modelling CH2Cl2 and CH3Cl combustion and/or pyrolysis, *Proc 24th Symp (Int) on Comb*, 743–8.
21. Ho, W. P., Barat, R. B. and Bozzelli, J. W., 1992, Thermal reactions of CH_2Cl_2 in H_2/O_2 mixtures: Implications for chlorine inhibition of CO conversion to CO_2, *Comb & Flame*, 88: 265–95.
22. Ho, W. P., Yu, Q. R. and Bozzelli, J. W., 1992, Kinetic study on pyrolysis and oxidation of CH_3Cl in Ar/H_2/O_2 mixtures, *Comb Sci & Tech*, 85 (1/6): 23–63.
23. Ho, W. P., Booty, M. R., Magee, R. S. and Bozzelli, J. W., 1995, Analysis and optimization of chlorocarbon incineration through use of a detailed reaction mechanism, *Ind & Eng Chem Res*, 34 (12): 4185–92.
24. Booty, M. R., Bozzelli, J. W., Ho, W. P. and Magee, R. S., 1995, Simulation of a three-stage chlorocarbon incinerator through the use of a detailed reaction mechanism—chlorine to hydrogen mole ratios below 0.15, *Env Sci & Tech*, 29 (12): 3059–63.
25. Rota, R., Bonini, F., Servida, A., Morbidelli, M. and Carra, S., 1994, Analysis of detailed kinetic schemes for combustion processes: Application to a methane-ethane mixture, *Chem Eng Sci*, 49 (24A): 4211–21.
26. Andrews, G. E. and Bradley, D., 1972, The burning velocity of methane-air mixtures. *Comb & Flame.* 19: 275–88.
27. Vagelopoulos, C. M., Egolfopoulos, F. N. and Law, C. K., 1994, Further considerations on the determination of laminar speeds with the counterflow twin-flow technique, *Proc 25th Symp (Int) on Comb*, 1341–7.
28. Drysdale, D. D., 1985, *An Introduction to Fire Dynamics* (John Wiley & Sons, New York).
29. Beyler, C., 1995, Flammability limits of premixed and diffusion flames, Chapters 2–9 in *SFPE Handbook of Fire Protection Engineering*, DiNenno, P. J., ed (NFPA, Quincy).
30. Hives, E. W. and Smith F. L., 1939, presented at *World Automotive Cong, New York, USA* (reprinted in 1940 in *SAE J, 46: 106–17).*
31. Atreya, A., Crompton, T. and Suh, J., 1994, *NIST Annual Conference for Fire Research*, NISTIR 5499, 67.
32. Dlugogorski, B. Z., Hichens, R. K. and Kennedy, E. M., 1997, Water vapour as an inerting agent, *Proc Halon Options Technical Working Conf, Albuquerque*, 7-18.

ACKNOWLEDGEMENTS

The authors sincerely thank Mr P. Robinson for help in constructing the experimental apparatus and for collecting the preliminary results, as well Mr C. Lebeda of the Technical University of Vienna for providing a copy of the original paper by Mache and Hebra.

ADDRESS

Correspondence concerning this paper should be addressed to Dr B. Z. Dlugogorski, Department of Chemical Engineering, University of Newcastle, New South Wales 2308, Australia. E-mail: cgbzd@alinga.newcastle.edu.au.

The manuscript was received 1 May 1997 and accepted for publication after revision 9 March 1998.